Projection of the future changes in tropical cyclone activity affecting East Asia over the western North Pacific based on multi-RegCM4 simulations

Jie Wu[1], Xuejie Gao[2], Ying Shi[3], Filippo Giorgi[4]

([1] Gannan Normal University, Ganzhou, 341000, China; [2] Climate Change Research Center, IAP, CAS, Beijing, 100049, China;[3] National Climate Center, CMA, Beijing, 100081, China;[4] The Abdus Salam International Center for Theoretical Physics, Trieste, 34100, Italy)

(gaoxuejie@mail.iap.ac.cn)

1. INTRODUTION

The frequency of TCs generated in the western North Pacific (WNP) is the largest compared to any other basin. TCs, particularly those making landfall, cause great damage to East Asia. Researchers use global climate models (GCMs) in climate change studies to simulate future changes in temperature, precipitation, etc. However, they are difficult to properly simulate small-scale weather and climate systems like TCs, due to their coarse resolutions. This means that they cannot capture all the dynamic processes within a TC. Recently, an unprecedented new set of 21st century climate change experiments using the regional climate model RegCM4 at 25 km grid spacing driven by 5 global models over the East Asia CORDEX domain was completed. This provides a good opportunity to conduct further studies on the topic of TCs in the WNP, and therefore, here we present an analysis of the projected changes in the genesis, track, intensity and landfall of TCs over the WNP based in this set of simulations.

2. MODEL, DATA AND METHODS

The regional climate model used in this study, RegCM4, was developed at the Abdus Salam International Center for Theoretical Physics (ICTP). The simulations were performed as part of Phase II of the CORDEX-East Asia domain at 25 km grid spacing. Initial and time evolving lateral boundary conditions are needed to drive the model, specifically for temperature, specific humidity, and wind (meridional and zonal components) at all vertical levels, as well as surface pressure and SST. These were interpolated from five different CMIP5 GCM outputs. The lateral boundary conditions scheme was carried out with an exponential relaxation technique (Giorgi et al., 1993), with a lateral buffer zone width of 12 grid points. The lateral boundary conditions and the prescribed SST were updated every 6 hours. The five driving CMIP5 GCMs are CSIRO-Mk3.6.0, EC-EARTH, HadGEM2-ES, MPI-ESM-MR and NorESM1-M. The ensemble mean of the 5 runs was derived using an equally weighted ensemble averaging method and is indicated by ensR.

Six-hourly best track data of observed TCs for model validation were obtained from the International Best Track Archive for Climate Stewardship (IBTrACS v03r10). The steering flow, which predominantly regulates the variation in TC tracks and landfall positions is defined as the average flow from 300 hPa to 850 hPa. An observational estimate was obtained from the ERA-Interim dataset with 1.5° × 1.5° resolution from June to September.

The software of TSTORMS (Detection and Diagnosis of Tropical Storms in High-Resolution Atmospheric Models) provided by Geophysical Fluid Dynamics Laboratory (https://www.gfdl.noaa.gov/tstorms/) is employed in the present study. The method uses the basin-, time-, and model-dependent vorticity. Based on the 6- hourly data, the TC detection procedure can be summarized as follows:

- The 850 hPa relative vorticity maximum in a centered 20 × 20 grid box exceeds the vorticity threshold.
- The local sea level pressure (SLP) minimum is considered as the TC center, and the distance of this TC center from the vorticity maximum must not exceed 2° longitude or latitude.
- The local maximum temperature averaged between 200 hPa and 500 hPa is defined as the warm core center, which should be within a radius of 2° longitude or latitude from the TC center. The temperature of warm core minus the averaged surrounding temperature must exceed the vertically integrated temperature anomaly threshold.
- The TC center at genesis should be over warm ocean points where the SST is higher than 26°C.

Then a trajectory analysis was per- formed to link the TC centers in time for a given track using the following procedure:

1) For each detected TC point, a check was performed to see if there were TCs during the following 6-hour period within a distance of 400 km.
2) If several candidates exist, the closest TC was considered as belonging to the same track as the initial one. If more than one possibility is found, the ones which were to the west and poleward of the current location were preferred.
3) To qualify as a TC trajectory, a TC needed to last for at least 1 day.

3. RESULTS

Fig.1 presents the TC tracks from the observations and simulations. The simulated TC tracks show general agree- ment with the observations, characterized by a motion towards the west first and then followed by a prevailing northwestward track. The track density in the simulations also agrees well with the observed except for NdR, which is characterized by much lower frequencies to the north and east of 135° E (Fig. 1f). An underestimation of the TC intensity is evident from the figure, with fewer strong typhoon (STY) and super typhon (SuperTY) compared to the observations.

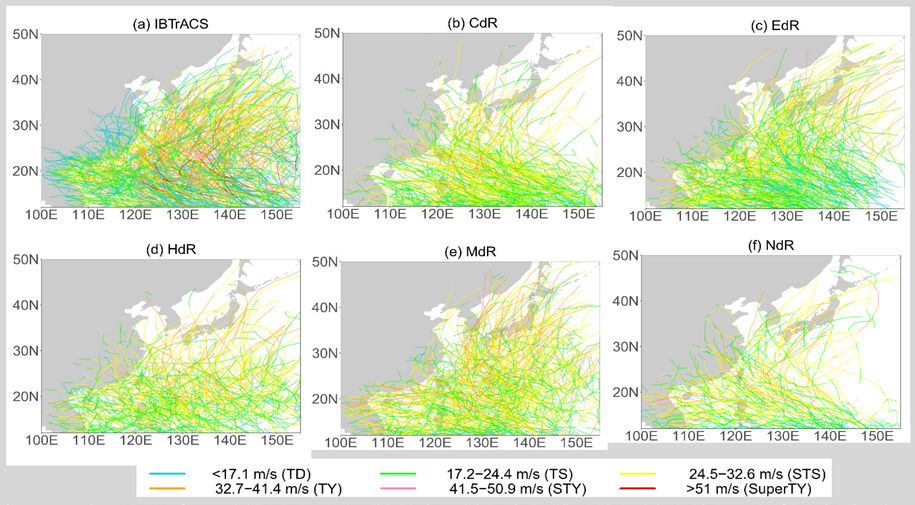

Fig. 1 TC tracks over the WNP from (a) IBTrACS, (b) CdR, (c) EdR, (d) HdR, (e) MdR and (f) NdR in the present-day period of 1986–2005. TC tracks are color coded based on the intensities of TCs (TD: tropical depression, TS: tropical storm, STS: strong tropical storm, TY: typhoon, STY: strong typhoon, and SuperTY: super typhoon).

Projected changes in the TC genesis frequency by the end of the 21st century (2079–98) from the individual simulations and ensR are presented in Fig. 2. In general, the change patterns show a mixture of increases and decreases. However, the increases are predominant in all of the five simulations. The increase of TC genesis frequency is dominant in ensR over the region, although with poor agreement at the individual grid box level among the simulations (Fig. 2f). The regional mean increase of TC genesis in ensR is 3.7 yr^{-1} (16%). The projected increase of TC genesis frequency may be due to the dominant favorable environment for TC formation, such as the increases of relative vorticity at 850 hPa, relative humidity at 700 hPa, etc.

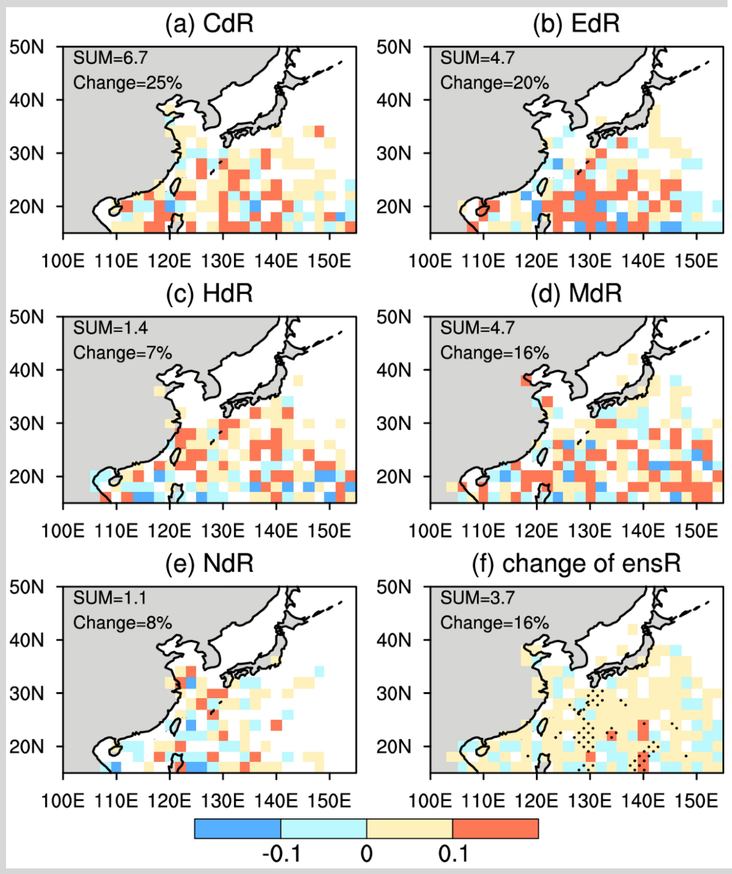

Fig. 2 Projected annual mean changes of genesis frequency (number per 2° × 2° square per year) from (a) CdR, (b) EdR, (e) HdR, (d) MdR, (e) NdR and (f) ensR over the WNP in the end of 21st century (2079–98, in relative to 1986–2005). Regional sums and the percentage of the changes are provided in the upper left corner of the panels. The dot in (f) indicates at least 4 out of 5 models agree on the sign of change.

Figure 3a compares the annual cycle of monthly mean TC genesis number between the present-day period of 1986–2005 and the end of the 21st century. The general characteristics of the seasonal evolution of the TC genesis remains unchanged, with a pronounced late summer maximum. General increases are found in most months except May and October (see also Fig. 3b). The increase is largest in August (1.33 mon^{-1}), followed by July (1.03 mon^{-1}) and September (0.62 mon^{-1}), with best cross-simulation agreement in August and September. The percentage increases are largest in January (47%) and August (42%), and substantial values are also found during February, June, July and September (16%–35%).

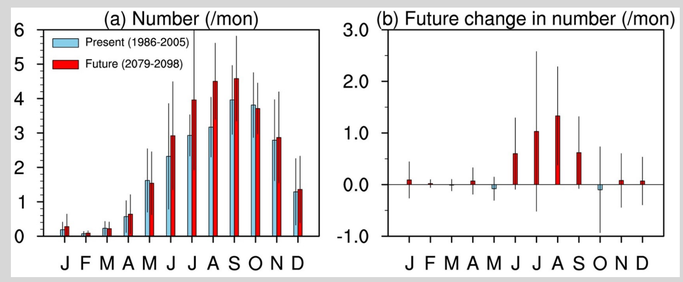

Fig. 3 Annual cycle of regional averaged TC (a) genesis frequency (number per month) during the present- day period of 1986–2005 (blue bars) and at the end of the 21st century (red bars) from ensR and (b) future change (number per month) over the WNP. The vertical lines indicate one standard deviation of the five simulations.

The future changes of TC occurrence frequency for the individual simulations and ensR are shown in Fig. 4. The changes show a general increase in four out of the five simulations, being most pronounced for CdR (regional mean of 0.20 yr^{-1}, or 28%). A mixture of negative-positive change is found in HdR, MdR, and NdR, with the regional mean showing increases ranging from 0.02–0.11 yr^{-1} (3%–16%). A broad decrease in the south and increase in the northeast is found for EdR, with the regional mean showing a decrease by 0.07 yr^{-1} (–9%). A general increase is found in ensR (Fig. 4f), more pronounced (>0.6 yr^{-1}) over the ocean east of Taiwan Island, south of Japan, and the region around (20°N, 140°E). The change over the tropical ocean at low latitudes shows larger areas of decrease, indicating a slight north-ward shift of the TC tracks in the future. Furthermore, a tendency for TCs penetrating further inland is evident. The increases are in good agreement among the simulations, with a regional mean of 0.06 yr^{-1} (10%).

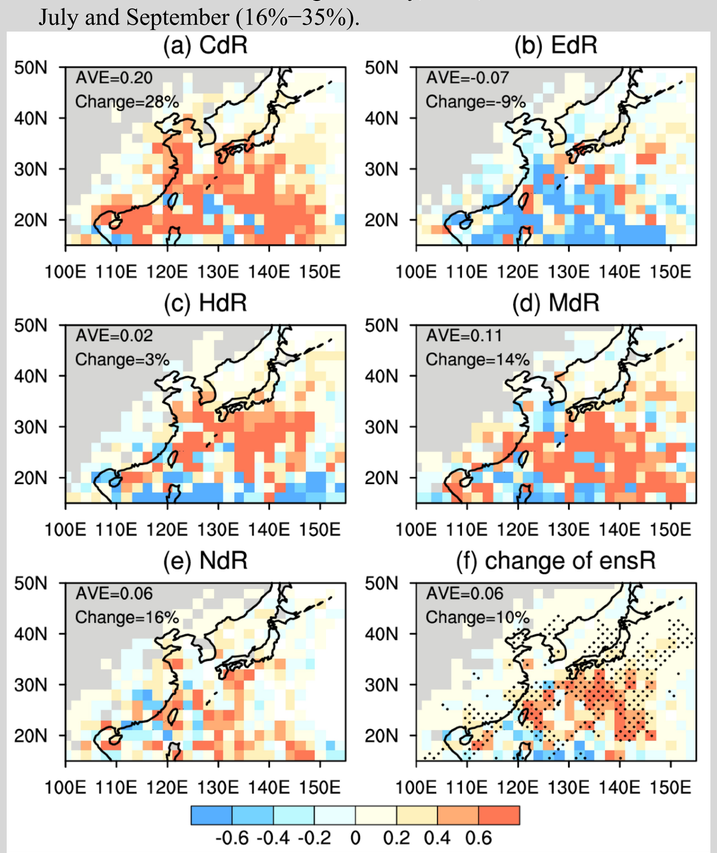

Fig. 4. Same as Fig. 2, but for occurrence frequency.

Percentages of TC duration, grades and minimum SLP for ensR and the spread of the simulations for the present- day period of 1986–2005 and at the end of the century periods are presented in Fig. 5. The duration of the TCs shows little change in the future (Fig. 5a), with a mix of positive and negative change found throughout the distribution. For example, an increase from 36% to 39% is found for the duration of 0–2 d, and a decrease from 17% to 14% for durations of 4–6 d. The spread is in general small among the simulations.

For the grades (Fig. 5b), we find a decrease in the low to mid-level TS and STS categories and an increase in the high end categories TY and STY, thus illustrating a distribution shift towards more intense tropical storms. In particular, the percentage of STY is almost doubled in the future compared to the present-day period (from 4% to 7%), indicating more intense TCs in the future. This result is confirmed by an increase in the percentage of minimum SLP in the categories less than 990 hPa and a decrease in the category higher than 990 hPa (Fig. 5c). Specifically, the percentage of TCs with minimum SLP less than 980 hPa increases from ~3% in the present-day period to ~5% in the future (~57% more), and with SLP less than 990 hPa from 14% for the present-day period to about 19% for the future (~31% more).

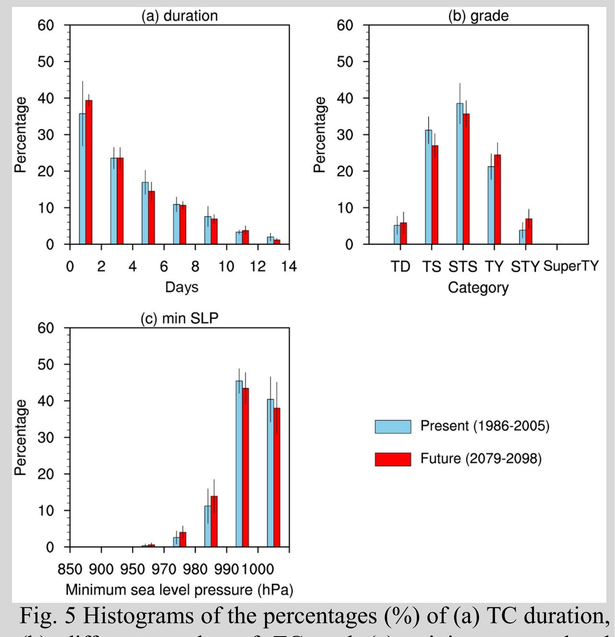

Fig. 5 Histograms of the percentages (%) of (a) TC duration, (b) different grades of TC and (c) minimum sea level pressure for ensR for the present-day period of 1986–2005 (blue bars) and at the end of the 21st century (red bars). The vertical lines indicate one standard deviation of the five simulations.

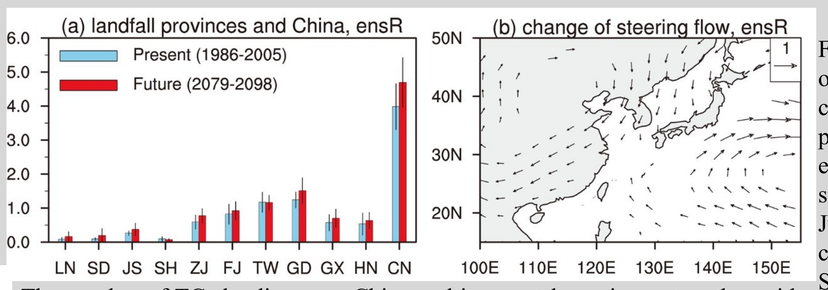

Fig. 6 (a) Histograms of annual mean number of landfall TCs (number per year) in the coastal provinces and whole of China for the present-day period of 1986–2005 and at the end of 21st century from ensR. (b) Changes of steering flow (vector; m s^{-1}) averaged from June to September for ensR at the end of 21st century, only shown those with $p<0.05$ (by the Student's *t*-test method). The vertical lines in (a) indicate one standard deviation of the five simulations. LN, SD, JS, SH, ZJ, FJ, TW, GD, GX, and HN represent Liaoning, Shandong, Jiangsu, Shanghai, Zhejiang, Fujian, Taiwan, Guangdong, Guangxi, and Hainan, respectively.

The number of TCs landing over China and its coastal provinces, together with the spread of the simulations, in the present-day period of 1986–2005 and at the end of the 21st century time-slices are shown in Fig. 6a. The number of landfalls is projected to increase in most of the coastal provinces in China, except the Shanghai City with its small size of area coverage. The largest increase is found over Guangdong (0.27 yr^{-1}) followed by Zhejiang (0.18 yr^{-1}) and Fujian (0.13 yr^{-1}). When measured by percentage, the increase is largest in Shandong (111%), followed by Liaoning (100%) in the north, and Jiangsu (42%) in the central coastal regions. The total number of TC landfalls over China increases from 3.98 yr^{-1} in the present-day period to 4.69 yr^{-1} (18% increase) at the end of the century. Figure 6b presents the change of steering flow at the end of 21st century. This is characterized by two anti-cyclonic circulations with centers located over the northern part of China and the western WNP, centered at (115°E, 40°N) and (155°E, 25°N), respectively. Both circulation changes contribute to a prevailing onshore flow for most of the Chinese mainland, which favors TC landing and thus leads to the higher number of landfall TCs.

4. CONCLUSIONS

1) The model captures the general features of the observed TC activity, although with slightly underestimated number of genesis events and underestimated number of occurrences, as a result of shorter than observed tracks. The model underestimates very intense TCs, likely due to the coarse resolution of most models , but shows good performance for medium intensity and intense TCs. Overall, the simulations underestimate the number of landfall TCs in most coastal regions of China.

2) An increase in the TC genesis by ~16% averaged over the analysis region is projected by the end of the 21st century. The change of occurrence frequency shows a general increase, with a regional mean value of 10%. A slight northward shift of the TC occurrence in the future is also found.

3) The intensity of the TCs, in particular for the percentage of intense ones, is projected to increase over the WNP, consistent with previous studies. In addition, more TC landfalls over most coastal provinces of China are projected, indicating increased risks associated to TCs for coastal areas.